On analyzing networks via curvature measures: review of methodologies and applications

Réka Albert, Nazanin Azarhooshang, Tanima Chatterjee, Bhaskar DasGupta, Prithviraj Sengupta, Aishi Agarwal, and Garima Kankariya

Abstract Suitable notions of shapes play a critical role in investigating objects in mathematics, physics and other research areas. Various kinds of curvatures are very natural measures of shapes of higher dimensional objects in mainstream physics and mathematics. However, any attempt to extend notions of these kinds of measures to networks needs to overcome several key challenges. In this article we review several curvature measures for networks such as ***(i)*** Gromov-hyperbolic curvature, ***(ii)*** extension of discretization of Ricci curvature for polyhedral complexes, and ***(iii)*** extension of discretization of Ricci curvature via mass transportation distances, and the corresponding flow technique. We finally review the bioinformatics applications

Réka Albert
Pennsylvania State University, Department of Physics, University Park, PA 16802, USA
e-mail: rza1@psu.edu

Nazanin Azarhooshang
University of Illinois Chicago, Department of Computer Science, Chicago, IL 60607, USA
e-mail: nazanin.azarhoushang@gmail.com

Tanima Chatterjee
Boston University, Center for Computing & Data Sciences, Boston, MA 02215, USA
e-mail: tanima1609@gmail.com

Bhaskar DasGupta
University of Illinois Chicago, Department of Computer Science, Chicago, IL 60607, USA
e-mail: bdasgup@uic.edu

Prithviraj Sengupta
University of Illinois Chicago, Department of Computer Science, Chicago, IL 60607, USA
e-mail: prithvi1096@gmail.com

Aishi Agarwal
Vernon Hills High School, Vernon Hills, IL, 60061, USA
e-mail: aishiagarwal11@gmail.com

Garima Kankariya
Indian Institute of Technology, New Delhi, Delhi 110016, INDIA
e-mail: gkankariya12@gmail.com

of these measures for several biological networks such as *E. coli* transcriptional network, metabolic network of *M. tuberculosis*, protein-protein interaction networks in humans and network of functional correlations between brain regions for *attention deficit hyperactivity disorder*.

1 Introduction

Useful insights for many complex systems are often obtained by representing them as networks and analyzing them using *network-theoretic* and *combinatorial* tools [34, 73, 2]. For analyzing networks, researchers have proposed and evaluated a number of established network measures such as *degree-based measures* (*e.g.*, degree distributions), *connectivity-based measures* (*e.g.*, clustering coefficients), *geodesic-based measures* (*e.g.*, betweenness centralities) and other more novel network measures such as in [27, 60, 3, 12].

The network measures of interest for this article are appropriate notions of "network curvature". Curvatures are very natural measures of properties of higher dimensional objects in mainstream physics and mathematics [18, 14]. However, any attempt to extend these kinds of measures to networks need to overcome many key challenges. For example, networks are *discrete* objects that do *not* necessarily have an associated natural geometric embedding. There are several ways previous researchers have attempted to formulate notions of curvatures of networks and other combinatorial objects. In this article we review the following three basic types of network curvatures and their applications to biological networks:

Gromov-hyperbolic curvature: This measure was first suggested by Gromov in a group theoretic context [51]. The measure was first defined for continuous metric space [18], but was later also adopted for networks. There is a large body of research works dealing with theoretical and empirical aspects of this measure, *e.g.*, see [18, 32, 33, 20, 13, 42, 23] for theoretical aspects, and see [4, 58, 83] for applications to real-world networks.

Forman-Ricci curvature: Another notion of curvature of a network can be obtained by extending Forman's discretization of Ricci curvature for (polyhedral or CW) complexes [41] to networks. Informally, the Forman-Ricci curvature is applied to networks by topologically associating components (subnetworks) of a given network with higher-dimensional objects. The topological association itself can be carried out several ways. Although formulated relatively recently, there are already a number of papers investigating these measures [97, 96, 106, 32, 88, 21].

Ollivier-Ricci curvature: The curvature measure is obtained by using Ollivier's discretization of Ricci curvature [80, 78, 79, 77]. For an informal understanding, consider transporting a infinitesimally small ball centered at a point of a manifold along a specific direction to measure the "distortion" of that ball due to

the shape of the surface. Ollivier's discretization provides appropriate network-theoretic analogs of such concepts.

Note that Gromov-hyperbolic curvature is a *global* measure in the sense that it assigns one scalar value to the entire network. *Au contraire*, both Ollivier-Ricci curvature and Forman-Ricci curvature assign a number to each edge of the given network, but the numbers are calculated in very *different* ways since they capture *different* metric properties of a Riemannian manifold; some comparative analysis of these two measures can be found in [21, 88]. Beyond these network curvatures measures, other notions of curvature have also been explored (*e.g.*, see [26]), but they will not be discussed in this article. For a recent survey of network geometry and its applications, the reader is referred to [16].

2 Basic Notations and Terminologies

We assume that the reader is familiar with standard concepts and terminologies of graph theory and algorithmic analysis. In this article the terms "graph" and "network" will be used interchangeably. Unless mentioned otherwise, all networks in this article are undirected, unweighted and connected. The notations $\overline{u,v}$ and $\text{dist}_H(u,v)$ will denote a *shortest path* and the *distance* between the nodes u and v in a network H, respectively. For a node u of network $H=(V,E)$, $\mathsf{Nbr}_H(u)=\{u\}\bigcup\{v\,|\,\{u,v\}\in E\}$ and $\deg_H(u)=|\,\mathsf{Nbr}_H(u)\setminus\{u\}\,|$ denote the *closed* neighborhood and the *degree* of u in H, respectively. For any *edge-weighted* graph $H=(V,E,w)$ with $w:E\mapsto\mathbb{R}^+\cup\{0\}$, $\text{wt-deg}_H(u)=\sum_{v:\{u,v\}\in E}w(u,v)$ denotes the *weighted* degree of node u in H. A hypergraph consists of a set V of nodes and a collection of non-empty subsets (called hyper-edges) of V. In a directed hypergraph each directed hyperedge is of the form $A\rightarrow B$ where A and B are non-empty subsets of V; A and B are called the tail and the head of the hyperedge, respectively. For a node u for a directed graph $G=(V,E)$, the in-neighbors and out-neighbors of u are the sets of nodes $\{v\,|\,v\rightarrow u\in E\}$ and $\{v\,|\,u\rightarrow v\in E\}$, respectively.

3 Curvature Definitions and Related Facts

3.1 Gromov-hyperbolic Curvature (Gromov-hyperbolicity)

This curvature measure is defined only for unweighted undirected graphs. There are three alternate but equivalent ways of defining Gromov-hyperbolic curvature for a network $G=(V,E)$, namely via geodesic triangles, via 4-node condition or via Gromov-product of nodes.

The most efficient algorithmic implementation for computing Gromov-hyperbolicity is obtained by using the original definition of Gromov using Gromov-product of

nodes [51]. Define the Gromov-product of two nodes u and v anchored at node x, denoted by $(u|v)_x$, as

$$(u|v)_x = \frac{1}{2} \times \Big(\text{dist}_G(u,x) + \text{dist}_G(v,x) - \text{dist}_G(u,v) \Big)$$

Based on the above definition, the value of Gromov-hyperbolicity $\delta(G)$ of a graph $G = (V,E)$ is defined as

$$\delta(G) = \max_{x,u,v,w \in V} \Big\{ \min \big\{ (u|w)_x,\, (v|w)_x \big\} - (u|v)_x \Big\} \tag{1}$$

A second way of defining Gromov-hyperbolicity via the 4-node conditions is used in many papers and books such as [3, 18]. This definition goes as follows. For a set of four nodes $\{u_1,u_2,u_3,u_4\}$, let $u_{\sigma_1},u_{\sigma_2},u_{\sigma_3},u_{\sigma_4}$ be a permutation of the indices of the nodes such that

$$\begin{aligned} \text{dist}_G\big(u_{\sigma_1},u_{\sigma_2}\big) + \text{dist}_G\big(u_{\sigma_3},u_{\sigma_4}\big) &\leq \overbrace{\text{dist}_G\big(u_{\sigma_1},u_{\sigma_3}\big) + \text{dist}_G\big(u_{\sigma_2},u_{\sigma_4}\big)}^{=\mathscr{M}_{u_1,u_2,u_3,u_4}} \\ &\leq \underbrace{\text{dist}_G\big(u_{\sigma_1},u_{\sigma_4}\big) + \text{dist}_G\big(u_{\sigma_2},u_{\sigma_3}\big)}_{=\mathscr{L}_{u_1,u_2,u_3,u_4}} \end{aligned}$$

Based on the above definition, the value of Gromov-hyperbolicity $\widehat{\delta}(G)$ of a graph $G = (V,E)$ is defined as

$$\widehat{\delta}(G) = \frac{1}{2} \times \max_{u_1,u_2,u_3,u_4 \in V} \big\{ \mathscr{L}_{u_1,u_2,u_3,u_4} - \mathscr{M}_{u_1,u_2,u_3,u_4} \big\} \tag{2}$$

A third way of of defining Gromov-hyperbolicity is via *geodesic triangles* [18]. A graph $G = (V,E)$ has a Gromov-hyperbolicity of $\widetilde{\delta}(G)$ if and only if $\widetilde{\delta}(G)$ is the minimum value such that for every ordered triple of shortest paths $(\overline{u,v},\overline{u,w},\overline{v,w})$, $\overline{u,v}$ lies in a $\widetilde{\delta}$-neighborhood of $\overline{u,w} \cup \overline{v,w}$, *i.e.*,

$$\widetilde{\delta}(G) = \min_{\substack{\alpha \in \mathbb{R} \\ (u,v,w) \in V \times V \times V}} \{ \alpha \,|\, \forall x \in \overline{u,v}\, \exists y \in \overline{u,w} \cup \overline{v,w} : \text{dist}_G(x,y) \leq \alpha \} \tag{3}$$

It is known that $\delta(G) = \widetilde{\delta}(G)$ and $\widehat{\delta}/c \leq \delta(G) \leq c\,\widehat{\delta}$ for some *universal* constant $c > 0$.

3.1.1 Forman-Ricci Curvature

Mathematically precise definitions of Forman-Ricci curvatures appear in references such as [32, 21, 22]. We here provide a succinct summary of these formalizations. We assume that the reader is familiar with basic topological concepts such

as faces, facets and simplexes; discussed in introductory topology textbooks such as [53, 44]. To use the formula suggested by Forman in [41] We define a partial order relation $\prec_{\mathfrak{f}}$ between faces of various dimensions of a simplex as follows: a ℓ-face $\mathfrak{f}^{\ell}$ is a parent of a ℓ'-face $\widehat{\mathfrak{f}}^{\ell'}$ (denoted by $\widehat{\mathfrak{f}}^{\ell'} \prec_{\mathfrak{f}} \mathfrak{f}^{\ell}$) if $\widehat{\mathfrak{f}}^{\ell'}$ is contained in $\mathfrak{f}^{\ell}$. Similarly, two ℓ-faces $\mathfrak{f}^{\ell}$ and $\widehat{\mathfrak{f}}^{\ell}$ are *parallel* (denoted by $\mathfrak{f}^{\ell} \parallel_{\mathfrak{f}} \widehat{\mathfrak{f}}^{\ell}$) if they have either at least one common *immediate predecessor* or at least one common *immediate successor* (in the partial order $\prec_{\mathfrak{f}}$) *but not both*.

To compute this kind of curvature, we use a topological association to glue nodes, edges, cliques and other subnetworks to form simplicial complexes, define a "weighting scheme" for these simplicial complexes, and then use the formula suggested by Forman in [41] for discrete Ricci curvature for (polyhedral or CW) simplicial complexes. There are many alternate ways such topological associations and weighting schemes can be performed. For concreteness, we describe the topological association rules as used in [32, 21, 22]; for other possible alternative associations the reader is referred to papers such as [15, 40, 104, 105].

To start the association, we topologically associate a q-simplex with a $(q+1)$-clique $\mathscr{K}_{q+1}$ (*e.g.*, 2-simplexes are associated with 3-cycles (triangles)). After this, an order d association f_d^p for every p-face f^p of a q-simplex is done with a subnetwork of at most d nodes that is obtained by starting with $\mathscr{K}_{p+1}$ and then *optionally* replacing each edge by a path between the two nodes (*e.g.*, f_d^2 for $d > 3$ is obtained from 3 nodes by connecting every pair of nodes by a path such that the total number of nodes in the subnetwork is at most d). *Naturally, the higher the values of p, q and d are, the more computationally intensive are the calculations of topological associations*.

A generic weighting scheme for these topological associations can be described in the following manner. Every node (0-simplex) and every edge (1-simplex) is assigned a weight of 1, every triangle (3-cycle or 2-complex) is assigned a weight based on the area of the triangle, and a polygon of p sides with $p > 3$ can be assigned a weight by first triangulating the polygon and then adding the weights of these triangles (*e.g.*, the weight of a non-degenerate 4-face is obtained by adding the weights of the 3-subfaces of this face). *We use the function $\rho(\cdot)$ to denote the weights of various sub-components in the following discussion*. Let d denote the order of the topological association used, and $e_{i,j}$ denote the edge $\{v_i, v_j\} \in E$. Using the CW-complex based Forman-Ricci curvature formula of [40], a 1-complex-based Forman's combinatorial Ricci curvature for an edge $e_{p,q} \in E$ in the given graph $G = (V, E)$ is given by [104]:

$$\mathfrak{C}_G^{1,d}(e_{p,q}) = \omega(e_{p,q}) \Bigg(\frac{\rho(v_p)}{\rho(e_{p,q})} + \frac{\rho(v_q)}{\rho(e_{p,q})} - \sum_{e_{p,j}, e_{i,q} \in E} \left(\frac{\rho(v_p)}{\sqrt{\left(\rho(e_{p,q})\rho(e_{p,j})\right)}} + \frac{\rho(v_q)}{\sqrt{\left(\rho(e_{p,q})\rho(e_{i,q})\right)}} \right) \Bigg) \quad (4)$$

However, since 1-complex based formula is a bit too simple and may not capture higher-order topological characteristics appropriate, papers such as [21, 105] use the following 2-complex based formula for the Forman-Ricci curvature of an edge $e \in E$ in the given graph $G = (V, E)$:

$$\mathfrak{C}_G^{2,d}(e) = \rho(e)\left[\left(\sum_{e\sim f_d^2}\frac{\rho(e)}{\rho(f_d^2)} + \sum_{v\sim e}\frac{\rho(v)}{\rho(e)}\right) - \sum_{e'||e}\left|\sum_{e',e\sim f_d^2}\frac{\sqrt{\rho(e)\rho(e')}}{\rho(f_d^2)} - \sum_{\substack{v\sim e\\ v\sim e'}}\frac{\rho(v)}{\sqrt{\rho(e)\rho(e')}}\right|\right] \quad (5)$$

In the above formula, for a node v, an edge e and a cycle $\mathscr{C}$, the notations $v \sim e$ and $e \sim \mathscr{C}$ indicate that v is an end-point of e and e is an edge of $\mathscr{C}$, respectively. A more general k-complex version of the curvature formula, leading to a definition of $\mathfrak{C}_G^{k,d}(e)$ for $k > 2$, can be derived by using the CW-complex based Forman-Ricci curvature formula of [40], but is of *limited* practical use.

Forman-Ricci curvature for an entire network

In some applications involving comparison of two networks in their entirety it may be preferable to have a single scalar value $\mathfrak{C}_G$ of Forman-Ricci curvature for the entire network G. This can be done based on the values of $\mathfrak{C}_G^{k,d}(e)$ values using curvature functions defined by Bloch [15], by using *Euler characteristics* or similar other methods. A simple Euler characteristics based scalar curvature, parameterized by p and d, defined in [32] for unweighted graphs is as follows.

$$\mathfrak{C}_G^{p,d} = \sum_{k=0}^{p}(-1)^k\left|\mathscr{F}_d^k\right| \quad (6)$$

where $\mathscr{F}_d^k$ is the set of all f_d^k's that are topologically associated as described before in this section. It is not difficult to see that $\mathfrak{C}_G^{2,d} = |V| - |E| + |\mathscr{C}_{d+1}|$ where $\mathscr{C}_{d+1}$ is the set of all cycles of *at most* $d+1$ nodes in G. Definitions of Forman-Ricci curvatures can be extended to (undirected, unweighted) hypergraphs, *e.g.*, see [61]; this has appeared to be very useful in applications to biological networks.

3.1.2 Ollivier-Ricci Curvature

This type of curvature was originally defined in publications such as [80, 78, 79, 77]. We here provide the definitions following the expositions in [8, 31]. Consider an edge $e = \{u, v\} \in E$ of our input (undirected unweighted) graph $G = (V, E)$. Let $\mathbb{P}_{\mathsf{Nbr}_G(u)}$ and $\mathbb{P}_{\mathsf{Nbr}_G(v)}$ denote the two uniform distributions over the nodes in

$$
\begin{array}{rl}
\textit{minimize} & \sum_{x\in \mathsf{Nbr}_G(u)} \sum_{y\in \mathsf{Nbr}_G(v)} \mathrm{dist}_G(x,y)\, z_{x,y} \\
\textit{subject to} & \sum_{y\in \mathsf{Nbr}_G(v)} z_{x,y} = \mathbb{P}_{\mathsf{Nbr}_G(u)}(x), \text{ for all } x \in \mathsf{Nbr}_G(u) \\
& \sum_{x\in \mathsf{Nbr}_G(u)} z_{x,y} = \mathbb{P}_{\mathsf{Nbr}_G(v)}(y), \text{ for all } y \in \mathsf{Nbr}_G(v) \\
& z_{x,y} \geq 0, \text{ for all } x \in \mathsf{Nbr}_G(u) \text{ and } y \in \mathsf{Nbr}_G(v)
\end{array}
$$

Fig. 1 The linear program, with the $z_{x,y}$'s as variables, whose optimal objective value is the quantity $\mathrm{EMD}_e(\mathbb{P}_{\mathsf{Nbr}_G(u)}, \mathbb{P}_{\mathsf{Nbr}_G(v)})$.

$\mathsf{Nbr}_G(u)$ and $\mathsf{Nbr}_G(v)$, respectively. The *earth mover's distance* $\mathrm{EMD}_e(\mathbb{P}_{\mathsf{Nbr}_G(u)}, \mathbb{P}_{\mathsf{Nbr}_G(v)})$ is the value of the objective function of an optimal solution of the linear program in Figure 1. The Ollivier-Ricci curvature $\mathfrak{C}_G(e)$ of the edge $e = \{u,v\}$ is then defined as

$$\mathfrak{C}_G(e) = 1 - \mathrm{EMD}_e(\mathbb{P}_{\mathsf{Nbr}_G(u)}, \mathbb{P}_{\mathsf{Nbr}_G(v)}) \tag{7}$$

If G is a graph with positive edge weights, the Ollivier-Ricci curvature is given by

$$\mathfrak{C}_G(e) = 1 - \frac{\mathrm{EMD}_e(\mathbb{P}_{\mathsf{Nbr}_G(u)}, \mathbb{P}_{\mathsf{Nbr}_G(v)})}{\mathrm{dist}_G(u,v)} \tag{8}$$

where the $\mathrm{dist}_G(\cdot,\cdot)$ values take the edge weights into consideration in calculating the shortest path. There are several modified definitions of the basic Ollivier-Ricci curvature as described above by ***(i)*** changing the distributions in $\mathbb{P}_{(\cdot)}$ from uniform to other non-uniform distributions [66, 10], ***(ii)*** by extending the "scopes" of the distributions $\mathbb{P}_{(\cdot)}$ from $\mathsf{Nbr}_G(u)$ and $\mathsf{Nbr}_G(v)$ to more subsets of nodes [75, 50], ***(iii)*** by changing $\mathrm{EMD}_e(\mathbb{P}_{\mathsf{Nbr}_G(u)}, \mathbb{P}_{\mathsf{Nbr}_G(v)})$ to other measures such as based on *displacement entropy* properties along geodesics [81] or based on volume growths [81], or ***(iv)*** a combination of the strategies in ***(i)***–***(iii)*** [50].

Some bioinformatics applications require the Ollivier-Ricci curvature from undirected graphs to directed graphs or hypergraphs. Several extensions have been proposed to extend Ollivier-Ricci curvature from graphs to (unweighted) directed graphs [108], to (unweighted) undirected hypergraphs [28, 7, 38, 1] and to (unweighted) directed hypergraphs [39]. For example, one relatively straightforward extension of Ollivier-Ricci curvature to a directed edge $u \to v$ in a directed graph would involve letting $\mathbb{P}_{\mathsf{Nbr}_G(u)}$ and $\mathbb{P}_{\mathsf{Nbr}_G(v)}$ be the two uniform distributions over the nodes in in-neighbors of u and out-neighbors of v, respectively, and letting $\mathrm{dist}_G(x,y)$ in Figure 1 denote the length of the shortest path from node x to node y.

4 Algorithmic and Computational Complexity Results

4.1 Computation of Gromov-hyperbolicity and Algorithmic Implications

Using (3) an exact calculation of $\widehat{\delta}(G)$ can be done by a straightforward approach in $O(n^4)$ time when n is the number of nodes. However, such a time is obviously prohibitive for very large n.

Faster exact and approximate computations of $\delta(G)$ can be done using the algorithm in [42], which we explain below. Let $V = \{u_1, \ldots, u_n\}$ be the set of nodes of G. Since $G = (V, E)$ is an unweighted undirected graph, using *breadth-first-search* we can compute in $O(n^3)$ time a $n \times n$ matrix $\mathscr{D}$ such that $\mathscr{D}[i, j] = \text{dist}_G(u_i, u_j)$. For any *fixed* node $u_\ell \in V$, let the quantity $\delta_\ell(G)$ be defined as

$$\delta_\ell(G) = \max_{u_i, u_j, u_k \in V} \Big\{ \min \big\{ (u_i|u_k)_{u_\ell}, (u_j|u_k)_{u_\ell} \big\} - (u_i|u_j)_{u_\ell} \Big\} \tag{9}$$

Thus, $\delta(G) = \max_{u_\ell \in V} \{\delta_\ell(G)\}$. Let ω be the *smallest* number such that two $t \times t$ matrices can be multiplied in $O(t^\omega)$ time for all $t > 1$ (as of writing this article, the value for ω is *about* 2.37286 [5]). For two $t \times t$ real matrices X and Y, the $(\max, \min)$-matrix multiplication $X \oplus Y$ of X and Y is defined as:

$$X \oplus Y[i, j] = \max_{k \in \{1, \ldots, t\}} \min \big\{ X[i, k], Y[k, j] \big\}$$

Duan and Pettie in [35] showed that $X \oplus Y$ can be computed in $O(t^{(3+\omega)/2}) \approx O(t^{2.688})$ time. To use the result in [35], Fournier, Ismail and Vigneron [42] observe that

$$\delta_\ell(G) = A_\ell \oplus A_\ell - A_\ell \tag{10}$$

where A_ℓ is the $n \times n$ matrix in which $A_\ell[i, j] = (u_i|u_j)_{u_\ell}$. Note that A_ℓ can be obtained from $\mathscr{D}$ in $O(n^2)$ time. Two time complexities for exact and approximate computations of $\delta(G)$ can now be obtained as follows:

- It is known [17] that $\delta_\ell(G) \leq \delta(G) \leq 2\delta_\ell(G)$ for any node $u_\ell \in V$. Thus, using (10) we immediately obtain an approximation of $\delta(G)$ within a factor of 2 in $O(n^{(3+\omega)/2}) \approx O(n^{2.688})$ time *excluding the time taken to compute the matrix* $\mathscr{D}$.
- Iterating the calculation in (10) for every $u_\ell \in V$ gives us an exact calculation of $\delta(G)$ in $n \times O(n^{(3+\omega)/2}) \approx O(n^{3.688})$ time.

If one is willing to allow *worse* approximation factors then further improvements in running times are possible, such as the following:

(*i*) Gromov [51] (see also [24, 47]) showed that G can be embedded in a tree in $O(n^2)$ time that such that the hyperbolicity value has an *additive* error of

$2\delta(G)\log_2 n$. That is, given a graph $G=(V,E)$ we can find in $O(n^2)$ time a tree $T=(V,E_T)$ such that $\text{dist}_G(u_i,u_j)-2\delta\log_2 n \leq \text{dist}_T(u_i,u_j) \leq \text{dist}_G(u_i,u_j)$ for any pair of nodes $u_i,u_j \in V$. Fournier, Ismail and Vigneron [42] showed that if one computes the value of $\alpha = \max_{u_i,u_j\in V}\{\text{dist}_G(u_i,u_j)-\text{dist}_T(u_i,u_j)\}$ in $O(n^2)$ time then α provides an approximation of $\delta(G)$ within a factor of $2\log_2 n$ in $O(n^2)$ time *excluding the time taken to compute the matrix* $\mathscr{D}$.

(ii) The result in ***(i)*** can be further improved by a different algorithm. Namely, Chalopin *et al.* [20] provides a 8-approximation of $\widehat{\delta}(G)$ in $O(n^2)$ time *excluding the time taken to compute the matrix* $\mathscr{D}$.

Algorithms for some computational problems may become more efficient if the input graph has small hyperbolicity. For example, routing-related problems, the diameter estimation problem or the bottleneck edge minimization problem may admit more efficient algorithms if the input graph has small hyperbolicity [25, 23, 24, 46, 33].

4.2 Computation of Forman-Ricci Curvature

Consider our input to be a graph $G=(V,E)$ with n nodes and m edges. $\mathfrak{C}_G^{1,d}(e_{p,q})$ can be calculated in $O(n+m)$ time using (4). A calculation of the value of $\mathfrak{C}_G^{2,d}(e)$ based on (5) has an worst-case running time of $O(n^{O(d)}$ and therefore may be infeasible for practical applications if n is large. The authors in [21] used the following simplified version of (5) that runs faster for For bioinformatics and other applications:

$$\mathfrak{C}_G^{2,d,\text{simplified}}(e)=\rho(e)\left[\left(\sum_{e\sim f_d^2}\frac{\rho(e)}{\rho(f_d^2)}+\sum_{v\sim e}\frac{\rho(v)}{\rho(e)}\right)-\sum_{\substack{e'||e\\ e',e\sim f_d^2}}\frac{\sqrt{\rho(e)\rho(e')}}{\rho(f_d^2)}\right] \quad (11)$$

With this modification, they were able to use the formula for computational purposes up to $d=5$.

Finally, it is possible to compute $\mathfrak{C}_G^{2,d}$ in $O(n^{O(d)})$ time using standard algorithmic techniques and data structures. The authors in [32] provided several algorithmic and computational complexity results on change-point detection in static and dynamic networks using $\mathfrak{C}_G^{2,d}$.

4.3 Computation of Ollivier-Ricci Curvature

Clearly, the computational complexity of computing $\mathfrak{C}_G(e)$ for a specific edge e is the same as that of computing $\text{EMD}_e(\mathbb{P}_{\mathsf{Nbr}_G(u)},\mathbb{P}_{\mathsf{Nbr}_G(v)})$, or equivalently that of

computing an optimal solution of the linear program in Figure 1. Using this observation the best time-complexity for computing $\mathfrak{C}_G(e)$ can be estimated as follows:

- $\mathfrak{C}_G(e)$ can be computed exactly in $O((\deg_G(u)+\deg_G(v))^{5/2})$ time using the algorithm for solving linear program in [62].
- If the input graph G is unweighted then, based on the results in [86, 37], for any $\varepsilon > 0$ we can compute, in $\tilde{O}\big(\frac{1}{\varepsilon^2}\deg_G(u)\deg_G(v)\big)$ time[1], an *additive* ε-*approximation* of $\mathfrak{C}_G(e)$, *i.e.*, a value α satisfying $\mathfrak{C}_G(e) \leq \alpha \leq \mathfrak{C}_G(e)+\varepsilon$.
- If the input graph G is unweighted then, based on the result in [8], one can compute in $O(\deg_G(u)+\deg_G(v))$ time a value α satisfying $1-3\,\alpha \leq \mathfrak{C}_G(e) \leq 1-\alpha$.

4.3.1 Query-based Local Algorithms for Efficient Computation of $\mathfrak{C}_G(e)$

The input graph for this section is an unweighted graph. The general idea behind these approaches is to exploit connections between distributed computing and random sampling to approximate *only* the optimal value of the objective function of an optimization problem with high probability [84, 9, 82]. Usually the sampling is done by picking a *small* number of suitable nodes or edges in the networks and querying their *local neighborhoods*. An additive ε-approximation of a quantity $\alpha \geq 0$ is obtained by computing a quantity β such that $\alpha \leq \beta \leq \alpha+\varepsilon$. Three standard query models that appear in the local algorithms literature for unweighted graphs (*e.g.*, see [84]) are as follows: the *node-pair* query model (query a pair of nodes to determine if an edge between them exists), the *neighbor* query model (query a node to obtain a *random not-yet-explored* adjacent node if it exists), and the *degree* query model (query a node to obtain its degree). However, the graph to query for our case is an *edge-weighted complete bipartite* graph $H = (A,B,w)$, where nodes in the left and right side of H are $A = \mathsf{Nbr}_G(u)$ and $B = \mathsf{Nbr}_G(v)$, and the weight of an edge $\{x,y\}$ ($x \in A, y \in B$) is $w(x,y) = \mathrm{dist}_G(x,y)$ (note that $w(x,y) \in \{1,2,3\}$ if $x \neq x$). This observation leads to the following natural extensions of the standard query models for our case [31]:

weighted node-pair query model: query a pair of nodes x,y to obtain the *weight* $w(x,y)$,

weighted degree query model: query a node x to obtain its *weighted* degree wt-$\deg_H(x)$,

weighted selective degree query model: query (x,a), where x is a node and $a \in \{1,2\}$ is a number, to obtain the number of edges of weight a that are incident on x, and

weighted neighbor query model: query (x,a), where x is a node and $a \in \{1,2\}$ is a number, to obtain a *random not-yet-explored* node v such that $w(u,v) = a$.

These local queries are implemented by a "distance oracle" that returns on demand the value of $w(x,y) = \mathrm{dist}_G(x,y)$ for two query nodes $x \in A$ and $y \in B$. The selection of a node or an edge as needed for a query is done by sampling via a suitable uniform distribution.

[1] The standard $\tilde{O}$ notation in algorithmic analysis hides poly-logarithmic terms, *e.g.*, terms like $\log^3 \deg_G(v)$.

DasGupta, Grigorescu and Mukherjee [31] provided several algorithmic and computational complexity results related to the above-mentioned query models for local algorithms in computing $\mathfrak{C}_G(e)$. In particular, they proved the following algorithmic result.

Theorem 1 ([31], paraphrased and rewritten in the context and notations of the current article). *For $j \in \{1,2\}$ let $\deg_{H,j}(x)$ denote the number of edges of weight j incident on node x in the graph H. Let $\delta > 0$ be any given constant. Then, we can design local algorithms with the following performance bounds:*

- *additive $(1+\varepsilon+\delta)$-approximation of $\mathfrak{C}_G(e)$ using $O(1)$ weighted neighbor queries*[2] *if $\max_x\{\deg_{H,1}(x)\} = O(1)$ and $\deg_G(v) \geq \deg_G(u) \geq (1-(\delta/3)) \times \deg_G(v)$,*
- *additive $\left(\frac{1}{2}+\varepsilon+\delta\right)$-approximation of $\mathfrak{C}_G(e)$ using $O(1)$ weighted neighbor queries*[3] *if $\max_x\{\deg_{H,1}(x)\} = O(1)$, $\max_x\{\deg_{H,2}(x)\} = O(1)$, and $\deg_G(v) \geq \deg_G(u) \geq (1-(\delta/3)) \times \deg_G(v)$.*

4.3.2 Normalized Ricci Flows and Modular Decomposition of Networks

For this section, the input graph $G = (V,E,w)$ is an edge-weighted graph where $w(e) \geq 0$ is the weight of an edge $e \in E$. *Informally*, in network research community a *module* (also sometimes called a *community* or *cluster*) of a network $G = (V,E)$ is a subset $V' \subset V$ of nodes that are connected *more* to nodes inside the module as opposed to nodes outside the module, and a *modular decomposition* [74, 63, 72, 30, 29] of the node set V is a partition of V into κ sets (modules) $V_1, \ldots, V_\kappa$ such that a node within a module is connected *more* to nodes inside its module as opposed to nodes outside the module. Such modular decompositions have a wide variety of applications [74, 72].

The concept of Ricci flow was originally introduced in the context of a Riemannian manifold by Hamilton [52] to provide a continuous change of the metric of the manifold One of the most ground-breaking application of this technique was done by Perelman [85] to solve the geometrization conjecture of Thurston on 3-manifolds. In the context of our edge-weighted network, this technique can be used to continuously change the weights of the edges of G. The original (*not* normalized) equation for these changes is the following:

$$w^{(t+1)}(e) = w^{(t)}(e) - w^{(t)}(e)\mathfrak{C}_G^{(t)}(e) \tag{12}$$

where $t = 0,1,2,\cdots$ is the discrete iteration index, $w^{(0)}(e) = w(e)$ for every edge $e \in E$, and $\mathfrak{C}_G^{(t)}(e)$ is the curvature value based on the edge-weights $W^{(t)} = \left\{ w^{(t)}(e) \,|\, e \in E \right\}$. Note that $w^{(t)}(e) \geq 0$ for all t since $\mathfrak{C}_G^{(t)}(e) \leq 1$ for all t. To apply this iterated method for modular decomposition of a network, the following two observations are crucial:

[2] The constant in $O(1)$ depends on the value of $\frac{1}{1-(\delta/3)}$.

[3] The constant in $O(1)$ depends on the value of $\frac{1}{1-(\delta/3)}$.

- Researcher works such as [75, 91] observe that removal of edges with highly negative curvature values is helpful for finding modules, *e.g.*, in the *precise* words of the authors in [91], "positively curved edges are well connected in the sense that none of them are essential for the proper transport operation and therefore positively curved edges naturally form a module".
- Generally speaking, the iterative process outlined in (12) should negatively reinforce weights of edges with negative curvatures and positively reinforce weights of edges with positive curvatures.

Based on these observations, a simple modular decomposition algorithm designed and evaluated by [75] based on Ricci flows is shown in Figure 2.

Input a positively edge-weighted graph $G = (V, E, w)$ and parameters ε, δ

Output a modular decomposition $V_1, \ldots, V_k$

Algorithm • execute the iterative process in (12)

until $|\mathfrak{C}_G^{(t+1)}(e) - \mathfrak{C}_G^{(t)}(e)| \leq \varepsilon$ for all e

• remove all edges e such that $w^{(t)}(e) \geq \delta$

• return each connected component as a module of G

Fig. 2 A modular decomposition algorithm designed by [75] based on un-normalized Ricci flows.

As observed in papers such as [59], there are problematic aspects to the Ricci flow equation in (12). Firstly, the sum of edge weights is not preserved in successive iterations. But, more importantly, there are networks for which the iterative process in (12) may result in all edges going to zero as t tends to infinity. To remedy these aspects, Lai, Bai and Lin [59] propose changing (12) as shown below such that the Ricci flow is "normalized" in the sense that the sum of edge weights remain the same and therefore *all* edge weights *cannot* become arbitrarily small:

$$w^{(t+1)}(e) = w^{(t)}(e) - w^{(t)}(e)\mathfrak{C}_G^{(t)}(e) + \frac{s\,w^{(t)}(e)}{\sum_{h\in E}\left(w^{(0)}(h)\mathfrak{C}_G^{(0)}(h)\right)} \sum_{h\in E}\left(w^{(t)}(h)\mathfrak{C}_G^{(t)}(h)\right) \tag{13}$$

In the above equation, $s > 0$ is some *constant* (called "step size" in [59]). Unfortunately, the following theorem shows that there are infinitely many graphs for which $w^{(1)}(e)$ will become negative thus rendering the iterative process in (13) impossible to execute beyond the first step.

Theorem 2. [89] *For all sufficiently large n, there exists a graph G_n on n nodes for which $w^{(1)}(f) < 0$ for some edge f of G_n.*

5 Applications of Network Curvatures in Bioinformatics and Neuroscience

By this time network curvature measures have been used in various applications in computer science and other inter-disciplinary areas. For example, many real-world networks (*e.g.*, preferential attachment networks, networks of high power transceivers in a wireless sensor network, communication networks at the IP layer and at other levels etc.) have been observed to have a *small* constant value of Gromov-hyperbolicity [76, 83, 56, 57, 6]. A small value of Gromov-hyperbolicity is often crucial for algorithmic designs; for example, several routing-related problems or the diameter estimation problem become easier for networks with small Gromov-hyperbolicity values [25, 23, 24, 46]. In this section, we discuss several applications of the curvature measures in the interdisciplinary area of computational biology.

5.1 Gromov-hyperbolic Curvatures to Study Biological Networks

A systematic study of the Gromov-hyperbolicity values for real biological networks and their corresponding implications was initiated in [4]. The authors in [4] computed Gromov-hyperbolicity values for the following 10 biological networks:

- two transcriptional regulatory networks, namely *E. coli* transcriptional [90] and *S. cerevisiae* transcriptional [71],
- five signalling networks, namely mammalian signaling [68], T-LGL signaling [109], *Drosophila* segment polarity [102], ABA signaling [64] and T cell receptor signalling [87],
- *C. elegans* metabolic network [55],
- immune response network [100], and
- oriented yeast PPI network [48].

They reported that the Gromov-hyperbolicity values of all except one network are small and statistically significant. They also reported several interesting experimentally-validated implications of these hyperbolicity values, such as

- Independent pathways that connect a signal to the same output node (*e.g.*, transcription factor) are rare, and if multiple pathways exist then they are interconnected through cross-talks.
- All the biological networks have central influential small-size node neighborhoods that can be selected to find knock-out nodes to cut off specific up- or down-regulation.

As an illustration of neuroscience applications, analysis of Gromov-hyperbolicity for brain-to-brain coordination networks are described in [99] and the references therein. The authors in [99] found that values of Gromov-hyperbolicities of their brain-to-brain coordination networks are indeed *small*, and were able to identify the subgraphs in these networks that contribute to small Gromov-hyperbolicity.

5.2 Ollivier-Ricci and Forman-Ricci Curvatures to Study Brain Disease Networks

Network analysis methods have been extensively used for studying properties of human brain networks [94, 93, 43, 70]. In this section we discuss the applications of discretized Ricci curvatures to study brain networks corresponding to two brain disorders.

5.2.1 Attention Deficit Hyperactivity Disorder

Attention deficit hyperactivity disorder (ADHD) is one of the most common neuro-developmental disorders of childhood impacting parts of the brain of approximately 11% of children and 5% of adults in the United States. The causes and risk factors for ADHD are still unknown, and as of yet there is no single clinical test that helps diagnose ADHD before its onset. There are several published neuroimaging studies that link the behavioral symptoms of ADHD to significant volume alteration in the brains of the patients with ADHD. For example:

- The statistical results of the neuroimaging studies of ADHD in Wang *et al.* [103] involving estimation of regional tissue volume changes showed significant volume reductions in the prefrontal, parietal and temporal regions, but significant volume enlargements in the occipital regions and posterial lateral ventricle.
- Sun *et al.* in [98] conducted a comparative study by building a model using anatomic and diffusion-tensor MRI of different regions of the brains of children with ADHD with that of children without the disease via MRI. They found that there were differences in the cortical shape of the frontal lobe and areas in the occipital lobe along with central cortex in the brains of ADHD patients with those in (age and sex-matched) control groups.

A functional correlation brain network of human brain is usually built by considering the different regions of a partition of the human brain, based on functional or anatomical properties [95], as nodes and defining the edges as functional correlations among these brain regions. Two prior graph theoretical studies of ADHD [65, 11] reported changes at the global level of the entire brain but did not study any altered connection patterns between different regions in the brain. The authors in [21] used the Forman-Ricci curvature to study such networks of functional correlations to detect statistically significant altered connection patterns between different regions of the brain caused by ADHD. The data for their analysis was collected from the *UCLA multimodal connectivity database* [19]. Their experimental results indicated 9 critical edges whose curvatures differ dramatically in brains of ADHD patients compared to healthy brains, and the importances of these edges were supported by existing neuroscience evidence [54, 69, 49, 98, 103]. In particular, their findings show that most of the extreme curvature changes happen in the *occipital cortex* and the *frontal cortex* regions of the brain.

5.2.2 Autism Spectrum Disorder

Autism spectrum disorder (ASD) results in altered white matter developmental patterns. Autologous cord blood infusion, a potential therapy, is believed to reduce neuro-inflammation and promote white matter development, thus triggering a reconfiguration of connectivity. Simhal *et al.* [92] used the Ollivier-Ricci curvature (for an undirected unweighted network) to identify the changes in the brain network after administering ASD patients a single infusion of autologous umbilical cord blood. They calculated the Spearman correlation between changes in clinical behavioral scores and changes in curvature following treatment, and identified a relationship between clinical improvement and altered curvature in three white matter pathways that are implicated in social and communication abilities.

5.2.3 Age-related Cognitive Decline

The study of age-related changes in brain networks is a fundamental pursuit in neuroscience. The authors in [107] used both Forman-Ricci curvature and Olliver-Ricci curvatures to quantify age-related alterations in resting state functional connectivity (brain) networks (rs-FCNs). rs-FCNs represent the interactions between different brain regions while at rest. The experiments were conducted on a participant pool of 225 individuals from two age groups: 153 young and 72 elderly persons. The authors used the following major steps:

- To begin, the authors preprocessed the raw resting-state functional magnetic resonance imaging scans of these subjects to divide the relevant regions of the brain into 200 brain activity regions using the Schaefer atlas, and, for each subject, computed correlations between each pair of these 200 regions to generate a 200×200 functional connectivity (FC) matrix to capture the strength of interactions between each pair.
- The FC matrices of the subjects were then used to construct their respective edge-weighted functional connectivity networks (FCNs) by implementing a two-step filtering approach.
  - First, the authors computed a maximum-weight spanning tree to identify the most significant and core connections that efficiently link different brain regions.
  - Next, they used a sparsity-based thresholding to sparsify the network by keeping only the strongest connections and discarding the weakest ones, resulting in an undirected and unweighted FCN of only highly correlated and connected nodes. This step ensured that the FCNs of each subject had an equal number of edges, thus allowing for a direct comparison of curvature measures across individuals. 49 different FCNs were constructed per individual to explore a range of edge densities and thresholds.

- To compare the FCNs between the young and elderly subjects, the authors calculated the average Forman-Ricci curvature and Oliver-Ricci curvature values for each edge.
- Finally, the authors used a two-tailed two-sample t-test at each edge density to evaluate the statistical significance of the difference in average edge curvature between the young and elderly subjects.

The authors found that the elderly group had higher average Forman-Ricci and Olliver-Ricci curvature values compared to the younger group. Using Neurosynth meta-analysis, the authors were also able to uncover cognitive and behavioral aspects linked to brain regions exhibiting different curvatures in young and elderly participants.

5.3 Forman-Ricci Curvatures for Directed Hypergraphs to Study E. coli Metabolic Networks

Escherichia Coli (*E. coli*) is a well-studied bacterium of immense importance in biotechnology and biomedicine. Study of the metabolism process of *E. coli* is important in uncovering the intricacies of cellular metabolism and gaining a deeper understanding of the essential pathways in the metabolic processes of this bacterium. Leal *et al.* [61] use a natural hypergraph to model the metabolism of *E. coli* and then apply Forman-Ricci curvature for directed hypergraphs to study the corresponding essential pathways. The metabolism of *E. coli* is represented as a directed hypergraph, where nodes represent metabolites and directed hyperedges $A \to B$ represent a chemical reaction where A and B are the starting materials and the products of the reaction, respectively[4]. The authors in [61] calculated the Forman-Ricci curvature for each hyperedge[5]. to quantify the bending and deviation from linearity of each reaction[6]. It is reported that the curvature values represent how indirect reactions are influenced by the degree of metabolites, and higher degrees of metabolites lead to higher curvature values since highly connected metabolites are involved in reactions with more intermediate steps, or bending[7]. Parts of the metabolic hypergraph of *E. coli* that display higher curvature values represent more abundance with reactions, suggesting presence of essential pathways in the metabolism process. The authors suggest that by separating these parts and studying them separately we should be

[4] Metabolites are small molecules that play important roles in chemical reactions and overall aid the function of *E. coli*.

[5] The concept of Forman-Ricci curvature for an edge is extended to a directed hyperedge by taking into consideration the incoming and outgoing edges at the tail and head of the edge, respectively. For further technical details, we refer the reader to [61].

[6] The actual pathway of a reaction is not necessarily a "straight line" that produces a direct output but in fact may involve many intermediate steps or "bends" in the journey, such as changes in the molecular structure of interactions between various molecules.

[7] Note that the degree of a metabolite is the number of connections it has in the metabolic hypergraph.

able to get a better understanding of the critical pathways in the metabolism of *E. coli*. ‘

5.4 Discrete Ricci Curvatures for Directed Graphs to Study M. tuberculosis Transcriptional Regulatory Network

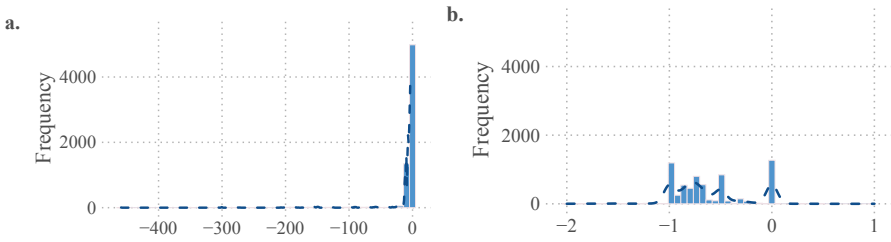

Fig. 3 (adopted from [38] with alterations) Distributions of the (**a**) Forman-Ricci curvatures, and (**b**) Ollivier-Ricci curvatures in the TRN of *M. tuberculosis*.

Eidi *et al.* [38] used both Forman-Ricci curvatures and Ollivier-Ricci curvatures for directed graphs to study the transcriptional regulatory network (TRN) of the human pathogen Mycobacterium Tuberculosis (*M. tuberculosis*) [36]. The TRN is constructed using ChIP-seq as a directed and unweighted network consisting of 2547 nodes, representing transcription factors, and 6581 directed edges representing regulatory interactions between transcription factors and target genes (for each directed edge, the transcription factor is the tail node and the corresponding target gene is the head node). The authors in [38] provide the following curvature analyses for this TRN:

- Figure 3(a) shows the distributions of the values of Forman-Ricci curvatures over all directed edges of the TRN of *M. tuberculosis*. The distribution shows a tall unimodal peak at zero, indicating that a significant amount of regulatory interactions between transcription factors and their target genes have a relatively straight or linear relationship. Most transcription factor nodes present in this TRN have smaller in-degrees and their target gene nodes also have smaller out-degrees. As a consequence, these transcription factor nodes and target gene nodes have limited reach and therefore not very influential in the TRN.
- Figure 3(b) shows the distributions of the values of Ollivier-Ricci curvatures over all directed edges of the TRN of *M. tuberculosis*. The distribution exhibits a multimodal pattern with peaks at curvature values of 0, -1, -0.5, and -0.75. This indicates that the regulatory interactions between transcription factor nodes and their corresponding target gene nodes have diverse curvature characteristics and therefore the TRN of *M. tuberculosis* is a complex and heterogeneous regulatory network.

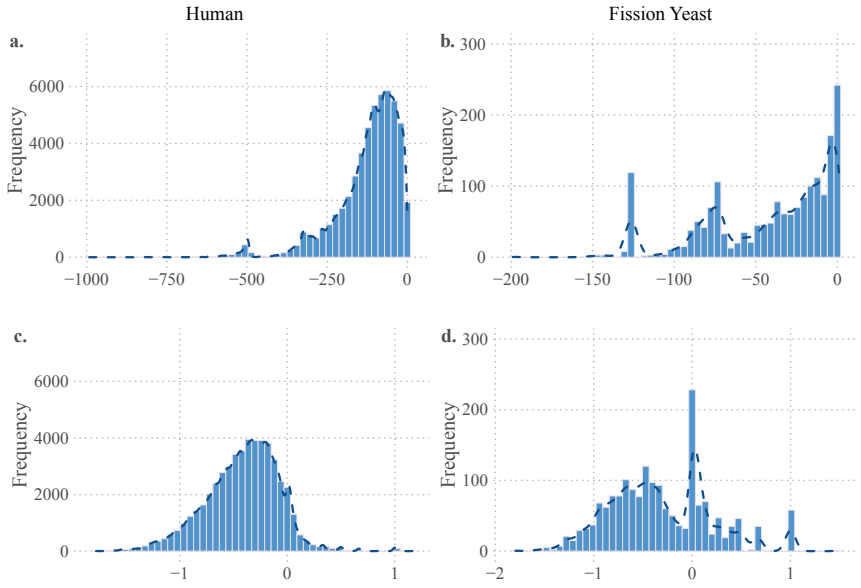

Fig. 4 (adopted from [38] with alterations) Distributions of the (**a**),(**b**) Forman-Ricci curvatures, and (**c**),(**d**) Ollivier-Ricci curvatures of the edges in the giant components in the PPI networks of human (left panel) and *S. pombe* (right panel).

5.5 Ollivier-Ricci and Forman-Ricci Curvatures to Study PPI Network

Eidi *et al.* [38] used both Forman-Ricci curvatures and Ollivier-Ricci curvatures to study PPI networks of humans with 8275 nodes and 52569 edges [67], and fission yeasts (*S. pombe*) with 1306 nodes and 2278 edges [101]. Both PPI networks are undirected and unweighted where nodes represent proteins and edges represent interactions. Eidi *et al.* [38] focused on the giant components of these networks, *i.e.*, the connected components of substantial size. They provided the following analyses for the Forman-Ricci curvature values of the edges in giant components for the human PPI networks:

- The bimodal distribution of Forman-Ricci curvature values in Figure 4(a) indicates that interactions within the giant component exhibit heterogeneity, with a major group of interactions clustered around a relatively small curvature value and a smaller group around a relatively high curvature value.
- The unimodal distribution of Ollivier-Ricci curvature values in Figure 4(c) suggests a relatively consistent pattern of these curvature values across the network.

For the giant components of the fission yeast PPI network, both the distributions in Figure 4(b),(d) are multimodal. They provided the following analyses for the curvature values of the edges in giant components for the fission yeast PPI networks:

- Figure 4(b) for Forman-Ricci curvature values shows a trimodal distribution, with the largest peak centered around a small-valued curvature. The two other peaks suggest the existence of multiple subsets or groups of protein interactions within the network, grouped by diverse levels of curvature. The peaks represent distinct clusters of interactions with varying degrees of bending or deviation from linearity.
- Figure 4(d) for Ollivier-Ricci curvature values shows another trimodal distribution, with a significant proportion of edges in the giant components of the network concentrated on a curvature value of zero. This suggests that a substantial number of protein interactions in the network display relatively little deviation from linearity. The other peaks, which occur at negative curvature values, imply the presence of interactions with significant bendings or deviations from linearity.

Overall, the fission yeast plots display a larger span of curvature values as opposed to the plot for the human PPI. This leads to a direct conclusion that the fission yeast PPI network is more disassortative than the human PPI network.

6 Conclusions

In this article we have discussed ideas from the exciting field of network curvature geometry that may lead to significant applications in several fields of computer science and other interdisciplinary areas. Some important characteristics of the curvature measures discussed in this article are that (*i*) they depend on non-trivial non-local network properties, and (*ii*) they often can be computed in polynomial time and therefore do not suffer from the curse of NP-completeness [45]. The references cited at various places in this article show that network curvature measures can encode non-trivial topological properties that are *not* expressed by more established network-theoretic measures such as degree distributions, clustering coefficients or betweenness centralities. We hope this article will motivate further collaboration between the researchers in network curvatures measures and other interdisciplinary areas.

References

1. T. Akamatsu. A new transport distance and its associated ricci curvature of hypergraphs. *Analysis and Geometry in Metric Spaces*, 10(1):90–108, 2022.
2. R. Albert and A.-L. Barabási. Statistical mechanics of complex networks. *Reviews of Modern Physics*, 74:47–97, 2002.
3. R. Albert, B. DasGupta, R. Hegde, G. S. Sivanathan, A. Gitter, G. Gürsoy, P. Paul, and E. Sontag. Computationally efficient measure of topological redundancy of biological and social networks. *Physical Review E*, 84:036117, 2011.
4. R. Albert, B. DasGupta, and N. Mobasheri. Topological implications of negative curvature for biological and social networks. *Physical Review E*, 89:032811, 2014.
5. J. Alman and V. V. Williams. A refined laser method and faster matrix multiplication. In *Proceedings of the thirty-second annual ACM-SIAM symposium on Discrete Algorithms*, pages 522–539. SIAM, 2021.
6. F. Ariaei, M. Lou, E. Jonckeere, B. Krishnamachari, and M. Zuniga. Curvature of sensor network: clustering coefficient. *EURASIP Journal on Wireless Communications and Networking*, 2008:213185, 2008.
7. S. Asoodeh, T. Gao, and J. Evans. Curvature of hypergraphs via multi-marginal optimal transport. In *2018 IEEE Conference on Decision and Control*, pages 1180–1185, 2018.
8. N. Azarhooshang, P. Sengupta, and B. DasGupta. A review of and some results for ollivier-ricci network curvature. *Mathematics*, 8(1416), 2020.
9. K. D. Ba, H. L. Nguyen, H. N. Nguyen, and R. Rubinfeld. Sublinear time algorithms for earth mover's distance. *Theory of Computing Systems*, 48(2):428–442, 2011.
10. S. Bai, A. Huang, L. Lu, and S.-T. Yau. On the sum of ricci-curvatures for weighted graphs. *Pure and Applied Mathematics Quarterly*, 17(5):1599–1617, 2021.
11. P. Barttfeld, A. Petroni, S. Báez, H. Urquina, M. Sigman, M. Cetkovich, T. Torralva, F. Torrente, A. Lischinsky, X. Castellanos, F. Manes, and A. Iba uez. Functional connectivity and temporal variability of brain connections in adults with attention deficit/hyperactivity disorder and bipolar disorder. *Neuropsychobiology*, 69(2):65–75, 2014.
12. D. S. Bassett, N. F. Wymbs, M. A. Porter, P. J. Mucha, J. M. Carlson, and S. T. Grafton. Dynamic reconfiguration of human brain networks during learning. *Proceedings of the National Academy of Sciences*, 118(18):7641–7646, 2011.
13. I. Benjamini. Expanders are not hyperbolic. *Israel Journal of Mathematics*, 108:33–36, 1998.
14. M. Berger. *A Panoramic View of Riemannian Geometry*. Springer-Verlag Berlin Heidelberg, 1 edition, 2003.
15. E. Bloch. Combinatorial ricci curvature for polyhedral surfaces and posets. *arXiv preprint arXiv:1406.4598*, 2014.
16. M. Boguñá, I. Bonamassa, M. De Domenico, S. Havlin, D. Krioukov, and M. Á. Serrano. Network geometry. *Nature Review Physics*, 3:114–135, 2021.
17. M. Bonk and O. Schramm. Embeddings of gromov hyperbolic spaces. *Geometric & Functional analysis GAFA*, 10:266–306, 2000.
18. M. R. Bridson and A. Häfliger. *Metric Spaces of Non-Positive Curvature*. Springer-Verlag Berlin Heidelberg, 1 edition, 1999.
19. J. Brown, D.R. Jeffery, A. Bandrowski, J.V. Horn, and S.Y. Bookheimer. The ucla multimodal connectivity database: A web-based platform for brain connectivity matrix sharing and analysis. *Frontiers in Neuroinformatics*, 6:28, 2012.
20. J. Chalopin, V. Chepoi, F. F. Dragan, G. Ducoffe, A. Mohammed, and Y. Vaxès. Fast approximation and exact computation of negative curvature parameters of graphs. *Discrete and Computational Geometry*, 65:856–892, 2021.
21. T. Chatterjee, R. Albert, S. Thapliyal, N. Azarhooshang, and B. DasGupta. Detecting network anomalies using forman-ricci curvature and a case study for human brain networks. *Scientific Reports*, 11, 2021.
22. T. Chatterjee, B. DasGupta, and R. Albert. A review of two network curvature measures. In T. M. Rassias and P. M. Pardalos, editors, *Nonlinear Analysis and Global Optimization*, volume 167 of *Springer Optimization and Its Applications*, pages 51–69. Springer, 2021.

23. V. Chepoi, F. Dragan, B. Estellon, M. Habib, and Y. Vaxès. Diameters, centers, and approximating trees of delta-hyperbolicgeodesic spaces and graphs. In *Proceedings of the Twenty-Fourth Annual Symposium on Computational Geometry*, SCG '08, pages 59–68, New York, NY, USA, 2008. Association for Computing Machinery.
24. V. Chepoi, F. F. Dragan, B. Estellon, M. Habib, Y. Vaxès, and Y. Xiang. Additive spanners and distance and routing labeling schemes for hyperbolic graphs. *Algorithmica*, 62:713–732, 2012.
25. V. Chepoi and B. Estellon. Packing and covering δ-hyperbolic spaces by balls. In M. Charikar, K. Jansen, O. Reingold, and J. Rolim, editors, *Approximation, Randomization, and Combinatorial Optimization. Algorithms and Techniques*, pages 59–73, Berlin, Heidelberg, 2007. Springer Berlin Heidelberg.
26. B. Chow and F. Luo. Combinatorial ricci flows on surfaces. *Journal of Differential Geometry*, 63(1):97–129, 2003.
27. V. Colizza, A. Flammini, M. Serrano, and A. Vespignani. Detecting rich-club ordering in complex networks. *Nature Physics*, 2:110–115, 2006.
28. C. Coupette, S. Dalleiger, and B. Rieck. Ollivier-ricci curvature for hypergraphs: A unified framework. *arXiv preprint arXiv:2210.12048*, 2023.
29. B. DasGupta. Computational complexities of optimization problems related to model based clustering of networks. In T. Rassias, C. Floudas, and S. Butenko, editors, *Optimization in Science and Engineering*, pages 97–113. Springer, New York, NY, 2014.
30. B. DasGupta and D. Desai. On the complexity of Newman's community finding approach for biological and social networks. *Journal of Computer and System Sciences*, 79(1):50–67, 2013.
31. B. DasGupta, E. Grigorescu, and T. Mukherjee. On computing discretized ricci curvatures of graphs: Local algorithms and (localized) fine-grained reductions. *Theoretical Computer Science*, 975:114127, 2023.
32. B. DasGupta, M. V. Janardhanan, and F. Yahyanejad. Why did the shape of your network change? (on detecting network anomalies via non-local curvatures). *Algorithmica*, 82(7):1741–1783, 2020.
33. B. DasGupta, M. Karpinski, N. Mobasheri, and F. Yahyanejad. Effect of gromov-hyperbolicity parameter on cuts and expansions in graphs and some algorithmic implications. *Algorithmica*, 80(2):772–800, 2018.
34. B. DasGupta and J. Liang. *Models and Algorithms for Biomolecules and Molecular Networks*. Wiley-IEEE Press, New Jersey, 2016.
35. R. Duan and S. Pettie. Fast algorithms for (max, min)-matrix multiplication and bottleneck shortest paths. In *Proceedings of the 2009 Annual ACM-SIAM Symposium on Discrete Algorithms*, pages 384–391, 2009.
36. N. C. Duarte, S. A. Becker, N. Jamshidi, I. Thiele, M. L. Mo, T. D. Vo, R. Srivas, and B. Ø. Palsson. Global reconstruction of the human metabolic network based on genomic and bibliomic data. *Proceedings of the National Academy of Sciences*, 104(6):1777–1782, 2007.
37. P. Dvurechensky, A. Gasnikov, and A. Kroshnin. Computational optimal transport: Complexity by accelerated gradient descent is better than by sinkhorn's algorithm. In J. Dy and A. Kraus, editors, *Proceedings of the 35th International Conference on Machine Learning*, volume 80 of *Proceedings of Machine Learning Research*, pages 1367—1376. PMLR, 10—15 Jul 2018.
38. M. Eidi, A. Farzam, W. Leal, A. Samal, and J. Jost. Edge-based analysis of networks: curvatures of graphs and hypergraphs. *Theory in Biosciences*, 139:337–348, 2020.
39. M. Eidi and J. Jost. Ollivier ricci curvature of directed hypergraphs. *Scientific Reports*, 10:12466, 2020.
40. R. Forman. Bochner's method for cell complexes and combinatorial Ricci curvature. *Discrete and Computational Geometry*, 29(3):323–374, 2003.
41. R. Forman. Bochner's method for cell complexes and combinatorial ricci curvature. *Discrete and Computational Geometry*, 29(3):323–374, 2003.
42. H. Fournier, A. Ismail, and A. Vigneron. Computing the gromov hyperbolicity of a discrete metric space. *Information Processing Letters*, 115(6):576–579, 2015.

43. L. K. Gallos, H. A. Makse, and M. Sigman. A small world of weak ties provides optimal global integration of self-similar modules in functional brain networks. *Proceedings of the National Academy of Sciences*, 109(8):2825–2830, 2012.
44. T. W. Gamelin and R. E. Greene. *Introduction to Topology*. Dover publications, 2 edition, 1999.
45. M. R. Garey and D. S. Johnson. *Computers and Intractability: A Guide to the Theory of NP-Completeness*. W. H. Freeman, 1 edition, 1979.
46. C. Gavoille and O. Ly. Distance labeling in hyperbolic graphs. In X. Deng and D.-Z. Du, editors, *Algorithms and Computation*, pages 1071–1079, Berlin, Heidelberg, 2005. Springer Berlin Heidelberg.
47. E. Ghys and P. Harpe. Sur les groupes hyperboliques d'après mikhael gromov. volume 83 of *Progress in Mathematics*, Boston, MA, USA, 1990. Birkhäuser.
48. A. Gitter, J. Klein-Seetharaman, A. Gupta, and Z. Bar-Joseph. Discovering pathways by orienting edges in protein interaction networks. *Nucleic Acids Research*, 39(4):e22–e22, 11 2010.
49. R. Gordji. An investigation of abnormal brain connectivity associated with regions implicated in adhd. Honors Theses 802, University of Mississippi, Sally McDonnell Barksdale Honors College, 2016.
50. A. Gosztolai and A. Arnaudon. Unfolding the multiscale structure of networks with dynamical ollivier-ricci curvature. *Nature Communications*, 12:4561, 2021.
51. M. Gromov. Hyperbolic groups. In S. M. Gersten, editor, *Essays in Group Theory*, volume 8, pages 75–263. Springer, New York, NY, 1987.
52. R. S. Hamilton. Three-manifolds with positive Ricci curvature. *Journal of Differential Geometry*, 17(2):255–306, 1982.
53. M. Henle. *A Combinatorial Introduction to Topology*. Dover publications, 1994.
54. T. Higo, R. B. Mars, E. D. Boorman, E. R. Buch, and M. F. S. Rushworth. Distributed and causal influence of frontal operculum in task control. *Proceedings of the National Academy of Sciences*, 108(10):4230–4235, 2011.
55. H. Jeong, B. Tombor, R. Albert, Z. N. Oltvai, and A.-L. Barabasi. The large-scale organization of metabolic networks. *Nature*, 407:651–654, 2000.
56. E. Jonckheere and P. Lohsoonthorn. Geometry of network security. In *Proceedings of the 2004 American Control Conference*, volume 2, pages 976–981, 2004.
57. E. Jonckheere, P. Lohsoonthorn, and F. Bonahon. Scaled gromov hyperbolic graphs. *Journal of Graph Theory*, 57(2):157–180, 2008.
58. E. Jonckheere, M. Lou, F. Bonahon, and Y. Baryshnikov. Euclidean versus hyperbolic congestion in idealized versus experimental networks. *Internet Mathematics*, 71:1–27, 2011.
59. X. Lai, S. Bai, and Y. Lin. Normalized discrete ricci flow used in community detection. *Physica A: Statistical Mechanics and its Applications*, 597:127251, 2022.
60. V Latora and M Marchiori. A measure of centrality based on network efficiency. *New Journal of Physics*, 9(6):188, jun 2007.
61. W. Leal, G. Restrepo, P. F. Stadler, and J. Jost. Forman-ricci curvature for hypergraphs. *Advances in Complex Systems*, 24(01):2150003, 2021.
62. Y. T. Lee and A. Sidford. Efficient inverse maintenance and faster algorithms for linear programming. In *2015 IEEE 56th Annual Symposium on Foundations of Computer Science*, pages 230–249, 2015.
63. E A. Leicht and M. E. J. Newman. Community structure in directed networks. *Physical Review Letters*, 100:118703, 2008.
64. S. Li, S. M. Assmann, and R. Albert. Predicting essential components of signal transduction networks: a dynamic model of guard cell abscisic acid signaling. *PLoS Biology*, 4(10):e312, 2006.
65. P. Lin, J. Sun, G. Yu, Y. Wu, Y. Yang, M. Liang, and X. Liu. Global and local brain network reorganization in attention-deficit/hyperactivity disorder. *Brain Imaging and Behavior*, 8(4):558–569, 2014.
66. Y. Lin, L. Lu, and S.-T. Yau. Ricci curvature of graphs. *Tohoku Mathematical Journal*, 63(4):605–627, 2011.

67. K. Luck, D. K. Kim, L. Lambourne, K. Spirohn, B. E. Begg, W. Bian, R. Brignall, T. Cafarelli, F. J. Campos-Laborie, B. Charloteaux, D. Choi, A. G. Coté, M. Daley, S. Deimling, A. Desbuleux, A. Dricot, M. Gebbia, M. F. Hardy, N. Kishore, J. J. Knapp, I. A. Kovács, I. Lemmens, M. W. Mee, J. C. Mellor, C. Pollis, C. Pons, A. D. Richardson, S. Schlabach, B. Teeking, A. Yadav, M. Babor, D. Balcha, O. Basha, C. Bowman-Colin, S. F. Chin, S. G. Choi, C. Colabella, G. Coppin, C. D'Amata, D. De Ridder, S. De Rouck, M. Duran-Frigola, H. Ennajdaoui, F. Goebels, L. Goehring, A. Gopal, G. Haddad, E. Hatchi, M. Helmy, Y. Jacob, Y. Kassa, S. Landini, R. Li, N. van Lieshout, A. MacWilliams, D. Markey, J. N. Paulson, S. Rangarajan, J. Rasla, A. Rayhan, T. Rolland, A. San-Miguel, Y. Shen, D. Sheykhkarimli, G. M. Sheynkman, E. Simonovsky, M. Tasan, A. Tejeda, V. Tropepe, J. C. Twizere, Y. Wang, R. J. Weatheritt, J. Weile, Y. Xia, X. Yang, E. Yeger-Lotem, Q. Zhong, P. Aloy, G. D. Bader, J. De Las Rivas, S. Gaudet, T. Hao, J. Rak, J. Tavernier, D. E. Hill, M. Vidal, F. P. Roth, and M. A. Calderwood. A reference map of the human binary protein interactome. *Nature*, 580(7803):402–408, 04 2020.
68. A. Ma'ayan, S. L. Jenkins, S. Neves, A. Hasseldine, E. Grace, B. Dubin-Thaler, N. J. Eungdamrong, G. Weng, P. T. Ram, J. J. Rice, A. Kershenbaum, G. A. Stolovitzky, R. D. Blitzer, and R. Iyengar. Formation of regulatory patterns during signal propagation in a mammalian cellular network. *Science*, 309(5737):1078–1083, 2005.
69. H. McCarthy, N. Skokauskas, A. Mulligan, G. Donohoe, D. Mullins, J. Kelly, K. Johnson, A. Fagan, M. Gill, J. Meaney, and T. Frodl. Attention network hypoconnectivity with default and affective network hyperconnectivity in adults diagnosed with attention-deficit/hyperactivity disorder in childhood. *JAMA Psychiatry*, 70(12):1329–1337, 2013.
70. D. Meunier, R. Lambiotte, and E. Bullmore. Modular and hierarchically modular organization of brain networks. *Frontiers in Neuroscience*, 4:200, 2010.
71. R. Milo, S. Shen-Orr, S. Itzkovitz, N. Kashtan, D. Chklovskii, and U. Alon. Network motifs: Simple building blocks of complex networks. *Science*, 298(5594):824–827, 2002.
72. M. E. J. Newman. Modularity and community structure in networks. *Proceedings of the National Academy of Sciences*, 103(23):8577–8582, 2006.
73. M. E. J. Newman. *Networks: An Introduction*. Oxford University Press, 03 2010.
74. M. E. J. Newman and M. Girvan. Finding and evaluating community structure in networks. *Physical Review E*, 69:026113, 2004.
75. C.-C. Ni, Y.-Y. Lin, F. Luo, and J. Gao. Community detection on networks with ricci flow. *Scientific Reports*, 9:9984, 2019.
76. Onuttom O. Narayan and I. Saniee. Large-scale curvature of networks. *Physical Review E*, 84:066108, Dec 2011.
77. Y. Ollivier. Ricci curvature of metric spaces. *Comptes Rendus Mathematique*, 345(11):643–646, 2007.
78. Y. Ollivier. Ricci curvature of markov chains on metric spaces. *Journal of Functional Analysis*, 256:810–864, 2009.
79. Y. Ollivier. A survey of ricci curvature for metric spaces and markov chains. In M. Kotani, M. Hino, and T. Kumagai, editors, *Advanced Studies in Pure Mathematics*, volume 57, pages 343–381. Mathematical Society of Japan, 2010.
80. Y. Ollivier. A visual introduction to Riemannian curvatures and some discrete generalizations. In G. Dafni, R. J. McCann, and A. Stancu, editors, *Analysis and Geometry of Metric Measure Spaces: Lecture Notes of the 50th Séminaire de Mathématiques Supérieures (SMS), Montréal, 2011*, volume 56, pages 197–219. American Mathematical Society, Providence, RI, USA, 2013.
81. Y. Ollivier and C. Villani. A curved brunn–minkowski inequality on the discrete hypercube, or: What is the ricci curvature of the discrete hypercube? *SIAM Journal on Discrete Mathematics*, 26(3):983–996, 2012.
82. K. Onak, D. Ron, M. Rosen, and R. Rubinfeld. A near-optimal sublinear-time algorithm for approximating the minimum vertex cover size. In *Proceedings of the twenty-third annual ACM-SIAM symposium on Discrete Algorithms*, pages 1123–1131. SIAM, 2012.

83. F. Papadopoulos, D. Krioukov, M. Boguna, and A. Vahdat. Greedy forwarding in dynamic scale-free networks embedded in hyperbolic metric spaces. In *2010 Proceedings IEEE INFOCOM*, pages 1–9, 2010.
84. M. Parnas and D. Ron. Approximating the minimum vertex cover in sublinear time and a connection to distributed algorithms. *Theoretical Computer Science*, 381(1):183–196, 2007.
85. G. Perelman. The entropy formula for the ricci flow and its geometric applications. *arXiv preprint arXiv:math/0211159v1*, 2002.
86. K. Quanrud. Approximating Optimal Transport With Linear Programs. In Jeremy T. Fineman and Michael Mitzenmacher, editors, *2nd Symposium on Simplicity in Algorithms (SOSA 2019)*, volume 69 of *OpenAccess Series in Informatics (OASIcs)*, pages 6:1—6:9, Dagstuhl, Germany, 2018. Schloss Dagstuhl–Leibniz-Zentrum fuer Informatik.
87. J. Saez-Rodriguez, L. Simeoni, J. A. Lindquist, R. Hemenway, U. Bommhardt, B. Arndt, U.-U. Haus, R. Weismantel, E. D. Gilles, S. Klamt, and B. Schraven. A logical model provides insights into t cell receptor signaling. *PLOS Computational Biology*, 3(8):e163, 2007.
88. A. Samal, R. P. Sreejith, J. Gu, S. Liu, E. Saucan, and J. Jost. Comparative analysis of two discretizations of ricci curvature for complex networks. *Scientific Reports*, 8:8650, 2018.
89. P. Sengupta, N. Azarhooshang, R. Albert, and B. DasGupta. Finding influential cores via normalized ricci flows in directed and undirected hypergraphs encoding biological and social interactions. *submitted to journal*.
90. S. S. Shen-Orr, R. Milo, S. Mangan, and U. Alon. Network motifs in the transcriptional regulation network of Escherichia coli. *Nature Genetics*, 31:64–68, 2002.
91. J. Sia, E. Jonckheere, and P. Bogdan. Ollivier-ricci curvature-based method to community detection in complex networks. *Scientific Reports*, 9:9800, 2019.
92. A. K. Simhal, K. L. H. Carpenter, S. Nadeem, J. Kurtzberg, A. Song, A. Tannenbaum, G. Sapiro, and G. Dawson. Measuring robustness of brain networks in autism spectrum disorder with Ricci curvature. *Scientific Reports*, 10:10819, 2020.
93. O. Sporns. The human connectome: a complex network. *Annals of the New York Academy of Sciences*, 1224(1):109–125, 2011.
94. O. Sporns. *Networks of the Brain*. The MIT Press, Cambridge, MA, 2016.
95. O. Sporns and R. F. Betzel. Modular brain networks. *Annual Review of Psychology*, 67(1):613–640, 2016.
96. R. P. Sreejith, J. Jost, E. Saucan, and A. Samal. Systematic evaluation of a new combinatorial curvature for complex networks. *Chaos, Solitons and Fractals*, 101:50–67, 2017.
97. R. P. Sreejith, K. Mohanraj, J. Jost, E. Saucan, and A. Samal. Forman curvature for complex networks. *Journal of Statistical Mechanics: Theory and Experiment*, 2016(6):063206, 2016.
98. H. Sun, Y. Chen, Q. Huang, S. Lui, X. Huang, Y. Shi, X. Xu, J. A. Sweeney, and Q. Gong. Psychoradiologic utility of mr imaging for diagnosis of attention deficit hyperactivity disorder: A radiomics analysis. *Radiology*, 287(2):620–630, 2017.
99. B. Tadić, M. Andjelković, and M. Šuvakov. Origin of hyperbolicity in brain-to-brain coordination networks. *Frontiers in Physics*, 6, 2018.
100. J. Thakar, M. Pilione, G. Kirimanjeswara, E. Harvill, and R. Albert. Modeling systems-level regulation of host immune responses. *PLOS Computational Biology*, 3(6):e109, 2007.
101. T. V. Vo, J. Das, M. J. Meyer, N. A. Cordero, N. Akturk, X. Wei, B. J. Fair, A. G. Degatano, R. Fragoza, L. G. Liu, A. Matsuyama, M. Trickey, S. Horibata, A. Grimson, H. Yamano, M. Yoshida, F. P. Roth, J. Pleiss, Y. Xia, and H. Yu. A proteome-wide fission yeast interactome reveals network evolution principles from yeasts to human. *Cell*, 164:310–323, 01 2016.
102. G. von Dassow, E. Meir, E.M. Munro, and G.M. Odell. The segment polarity network is a robust developmental module. *Nature*, 406:188–192, 2000.
103. J. Wang, T. Jiang, Q. Cao, and Y. Wang. Characterizing anatomic differences in boys with attention-deficit/hyperactivity disorder with the use of deformation-based morphometry. *American Journal of Neuroradiology*, 28(3):543–547, 2007.
104. M. Weber, J. Jost, and E. Saucan. Forman-ricci flow for change detection in large dynamic data sets. *Axioms*, 5(4), 2016.
105. M. Weber, E. Saucan, and J. Jost. Can one see the shape of a network? *arXiv preprint arXiv:1608.07838*, 2016.

106. M. Weber, E. Saucan, and J. Jost. Characterizing complex networks with forman-ricci curvature and associated geometric flows. *Journal of Complex Networks*, 5(4):527–550, 2017.
107. Y. Yadav, P. Elumalai, N. Williams, J. Jost, and A. Samal. Discrete ricci curvatures capture age-related changes in human brain functional connectivity networks. *Frontiers in Aging Neuroscience*, 15, 2023.
108. T. Yamada. The ricci curvature on directed graphs. *Journal of the Korean Mathematical Society*, 56(1):113–125, 2019.
109. R. Zhang, M. V. Shah, J. Yang, S. B. Nyland, X. Liu, J. K. Yun, R. Albert, and T. P. Loughran. Network model of survival signaling in large granular lymphocyte leukemia. *Proceedings of the National Academy of Sciences*, 105(42):16308–16313, 2008.